PHYSICAL REVIEW A **82**, 022311 (2010)

Efficient multimode quantum memory based on photon echo in an optimal QED cavity

Sergey A. Moiseev,[1,2,3,*] Sergey N. Andrianov,[2,3] and Firdus F. Gubaidullin[1,2]

[1]*Kazan Physical-Technical Institute of the Russian Academy of Sciences, 10/7 Sibirsky Trakt, Kazan RU-420029, Russia*

[2]*Institute for Informatics of Tatarstan Academy of Sciences, 20 Mushtary, Kazan RU-420012, Russia*

[3]*Physical Department of Kazan State University, Kremlevskaya 18, Kazan RU-420008, Russia*

(Received 8 April 2010; published 11 August 2010)

Effective multimode photon echo quantum memory on multiatomic ensemble in the QED cavity is proposed. We obtain the analytical solution for the quantum memory efficiency that can be equal to unity when optimal conditions for the cavity and atomic parameters are held. Detailed analysis of the optimal conditions is performed. Numerical estimation for realistic atomic and cavity parameters demonstrates the high efficiency of the quantum memory for an optically thin resonant atomic system that opens a door for real applications.

DOI: 10.1103/PhysRevA.82.022311 PACS number(s): 03.67.−a, 42.50.Pq, 42.50.Ct, 42.50.Md

I. INTRODUCTION

Quantum communications and quantum computation require an effective quantum memory (QM) that must be of a multimode and high fidelity character [1–5]. Most well-known electromagnetically induced transparency (EIT) based QM [6] demonstrates an efficient storage and retrieval only for a specific single temporal mode regime [7–9]. Photon echo QM [10–14] offers the most promising properties for a realization of the multimode QM [15–17]. However, the quantum efficiency of all discussed multimode variants of the photon echo QM tends to unity for infinite optical depth αL as $[1-\exp(-\alpha L)]^2$, where α and L are the resonant absorption coefficient and length of the medium along the light field propagation [18,19]. Above formula for QM efficiency imposes a fundamental limit for the QM efficiency so it is necessary to increase either the atomic concentration or the medium length. However, the QM device should be compact and the large increase of the atomic concentration gives rise to atomic decoherence due to the dipole-dipole interactions limiting thereby a storage time. So, using the free space QM scheme is quite problematic for practical devices.

Efficient QM on a multiatomic system inside the optical resonator has been considered on EIT effects in [20,21]. Possibility of the photon echo signal enhancement in resonator was demonstrated in [22]. Efficient photon echo QM with controlled reverse of inhomogeneous broadening (CRIB) has been studied recently in the ideal cavity [23] and in the bad cavity [24] where high QM efficiency has been demonstrated only for a specific optimal single mode regime. Here, we propose a general approach for a multimode photon echo type of QM in the QED cavity (single mode resonator). We demonstrate a high efficiency of the QM for the optimized system of atoms and QED cavity at arbitrary temporal shape of the stored field modes. We find a simple analytical solution for QM efficiency and the optimal conditions for a matching of the atomic and cavity parameters where the QM efficiency can reach unity even for a small optical depth of the medium inside the cavity.

*samoi@yandex.ru

II. BASIC EQUATIONS

We analyze a resonant multiatomic system in an arbitrary single mode one-sided QED cavity coupled with signal and bath field modes (nonsignal free space electromagnetic modes in our model). By following the cavity mode formalism [25], we use a Tavis-Cumming Hamiltonian [26] $\hat{H}=\hat{H}_o+\hat{H}_1$, for N atoms, field modes and their interactions taking into account the inhomogeneous and homogeneous broadenings of the atomic frequencies and continuous spectral distribution of the field modes where

$$\hat{H}_o=\hbar\omega_o\left\{\sum_{j=1}^{N}\hat{S}_z^j+\hat{a}^\dagger\hat{a}+\sum_{l=1}^{2}\int\hat{b}_l^\dagger(\omega)\hat{b}_l(\omega)d\omega\right\}\qquad(1)$$

are main energies of atoms (S_z^j is a z projection of the spin $1/2$ operator), the energy of the cavity field ($\hat{a}^\dagger$ and $\hat{a}$ are arising and decreasing operators), energies of signal ($l=1$) and bath ($l=2$) fields ($b_l^\dagger$ and b_l are arising and decreasing operators of the field modes $[\hat{b}_l^\dagger(\omega'),\hat{b}_{l'}(\omega)]=\delta_{l,l'}\delta(\omega'-\omega)$),

$$\begin{aligned}\hat{H}_1=&\hbar\sum_{j=1}^{N}[\Delta_j(t)+\delta\Delta_j(t)]\hat{S}_z^j\\&+\hbar\sum_{l=1}^{2}\int(\omega-\omega_o)\hat{b}_l^{+}(\omega)\hat{b}_l(\omega)d\omega\\&+i\hbar\sum_{j=1}^{N}[g_j\hat{S}_-^j\hat{a}^\dagger-g_j^*\hat{S}_+^j\hat{a}]\\&+i\hbar\sum_{l=1}^{2}\int\kappa_l(\omega)[\hat{b}_l(\omega)\hat{a}^\dagger-\hat{b}_l^\dagger(\omega)\hat{a}]d\omega.\end{aligned}\qquad(2)$$

The first term in (2) comprises the perturbation energies of atoms where $\Delta_j(t)$ is a controlled frequency detuning of jth atom $\Delta_j(t<\tau)=\Delta_j$ and $\Delta_j(t>\tau)=-\Delta_j$, $\delta\Delta_j(t)$ is its fluctuating frequency detuning determined by local stochastic fields, g_j is a photon-atom coupling constant in the QED cavity, S_+^j and S_-^j are the transition spin operators. Ensemble distributions over the detunings Δ_j and $\delta\Delta_j(t)$ determine inhomogeneous $\Delta_{\rm in}$ and homogeneous γ_{21} broadenings of the resonant atomic line. In the following, we use a Lorentzian shape for inhomogeneous broadening (IB) and a typical anzatz for the ensemble average over the fluctuating detunings $\delta\Delta_j(t)$:

$$\sum_{j=1}^{N}|g_j|^2\exp\{-i\Delta_j(t-t')\}\Phi_j(t,t') \equiv N|\bar{g}|^2\exp\{-(\Delta_{\rm in}+\gamma_{21})|t-t'|\}, \quad (3)$$

where $\Phi_j(t,t')=\exp\{-i\delta\varphi_j(t,t')\}$, $\delta\varphi_j(t,t')=\int_{t'}^{t}dt''\delta\Delta_j(t'')$, $|\bar{g}|^2$ is quantity averaged over the atoms. The second term in (2) contains frequency detunings of the lth field modes. The third term is the interaction energy of atoms with cavity mode. The fourth term is an interaction energy of the cavity mode with the signal and bath modes characterized by the coupling constants $\kappa_l(\omega)$. The coupling of the cavity mode with bath modes describes the nonideal character of the resonator.

We note that $[\hat{H}_o,\hat{H}_1]=0$ so a total number of excitations in the atomic system and the field modes is conserved during the quantum evolution, $\hat{H}_o$ makes a contribution only to the common phase of the wave function. H_1 determines a unitary operator $\hat{U}_1(t)=\exp\{-i\hat{H}_1t/\hbar\}$ causing the evolution of the atomic and field systems with a dynamical exchange and entanglement of the excitations among them. We assume that initially all atoms ($j=1,2,\dots,N$) stay in the ground state $|g\rangle_a=|g_1,g_2,\dots,g_N\rangle$ and we launch a signal multimode single photon field prepared in the initial quantum state $|\psi_{\rm in}(t)\rangle_{ph}=\prod_{k=1}^{M}\hat{\psi}_k^+(t-\tau_k)|0\rangle$, $\hat{\psi}_k^+(t-\tau_k)=\int_{-\infty}^{\infty}d\omega_k f_k(\omega_k)\exp\{-i\omega_k(t-\tau_k)\}\hat{b}_1^+(\omega_k)$; f_k is a wave function in the frequency space normalized for pure single photon state $\int_{-\infty}^{\infty}d\omega_k|f_k(\omega_k)|^2=1$, M is a number of modes, $|0\rangle$ is a vacuum state of the field. The kth photon mode arrives in the circuit at time moment τ_k, time delays between the nearest photons are assumed to be large enough $(\tau_k-\tau_{k-1})\gg\delta t_k$, δt_k is a temporal duration of the kth field mode. Additional bath field modes ($l=2$) are assumed to be in the vacuum state $b_2(\omega)|0\rangle=0$. Thus, the total initial state of the multimode light field and atoms is given by $|\Psi_{\rm in}(t)\rangle=|\psi_{\rm in}(t)\rangle_{ph}|g\rangle_a$.

Neglecting a population of excited atomic states and using the input and output field formalism [25] we derive the following linearized system of Heisenberg equations for the field operators and for the atomic operators in the rotating frame representation:

$$\frac{d}{dt}\hat{b}_l(\omega)=-i(\omega-\omega_0)\hat{b}_l(\omega)-\kappa_l(\omega)\hat{a}, \quad (4)$$

$$\frac{d}{dt}\hat{S}_-^j=-g_j^*\hat{a}-i[\Delta_j+\delta\Delta_j(t)]\hat{S}_-^j, \quad (5)$$

$$\frac{d}{dt}\hat{a}=\sum_{j=1}^{N}g_j\hat{S}_-^j-\tfrac{1}{2}(\gamma_1+\gamma_2)\hat{a}+\sqrt{\gamma_1}\hat{b}_1(t)+\sqrt{\gamma_2}\hat{b}_2(t), \quad (6)$$

where $\gamma_l=2\pi\kappa_l^2(\omega_o)$, $(l=1,2)$ [25]. The input signal field containing M temporally separated photon modes is given by $\hat{b}_1(t)=\sum_{k=1}^{M}\hat{b}_{1,k}(t-\tau_k)$, where $\hat{b}_{l,k}(\tilde{\tau}_k)=\frac{1}{\sqrt{2\pi}}\int_{-\infty}^{\infty}d\omega\exp\{-i(\omega-\omega_0)\tilde{\tau}_k\}\hat{b}_l(\omega)$ and obviously we have $\hat{b}_2(t)|0\rangle=0$.

III. QUANTUM STORAGE

By taking into account a formal solution of Eq. (5)

$$\hat{S}_-^j(t)=\hat{S}_-^j(t_o)\Phi_j(t,t_o)\exp\{-i\Delta_j(t-t_o)\} - g_j^*\int_{t_o}^{t}dt'\Phi_j(t,t')\exp\{-i\Delta_j(t-t')\}\hat{a}(t'), \quad (7)$$

we use the Laplace transformation for $\hat{a}_L(p)=\int_{t_0}^{\infty}dte^{-p(t-t_0)}\hat{a}(t)$ and similarly for $\hat{b}_{1,L}(p)$ in (6) that leads to $\hat{a}_L(p)=\sum_{n=1}^{4}\hat{a}_{n,L}(p)$, where

$$\hat{a}_{1,L}(p)=f(p)\hat{a}(t_o), \quad (8)$$

$$\hat{a}_{2,L}(p)=f(p)\sum_{j=1}^{N}g_j\hat{S}_-^j(t_o)\Phi_j^{(s)}(p), \quad (9)$$

$$\hat{a}_{3,L}(p)=f(p)\sqrt{\gamma_2}\hat{b}_{2,L}(p), \quad (10)$$

$$\hat{a}_{4,L}(p)=f(p)\sqrt{\gamma_1}\hat{b}_{1,L}(p), \quad (11)$$

where $\Phi_j^{(s)}(p)=\int_{t_o}^{\infty}dt\exp\{-(p+i\Delta_j)(t-t_o)\}\Phi_j(t,t_o)$, $\hat{b}_{l,L}(-i\omega)=\sqrt{2\pi}\hat{b}_l(\omega)$,

$$f(p)=\left(p+\frac{(\gamma_1+\gamma_2)}{2}+\frac{N_1|\bar{g}|^2}{(p+\Delta_{\rm in}+\gamma_{21})}\right)^{-1}. \quad (12)$$

After inverse Laplace transformation, we find a solution $\hat{a}(t)=\sum_{n=1}^{4}\hat{a}_n(t)$, where four terms of the cavity field $\hat{a}_n(t)=\frac{1}{2\pi}\int_{\varepsilon-i\infty}^{\varepsilon+i\infty}dpe^{p(t-t_0)}\hat{a}_{n,L}(p)$ have different temporal and physical properties. The first field $\hat{a}_1(t)$ is determined by the initial field $\sim\hat{a}_1(t_0)$ that disappears rapidly in the cavity on time interval $(t-t_o)>[\frac{1}{2}(\gamma_1+\gamma_2)+N_1|\bar{g}_1|^2/(\Delta_{\rm in}+\gamma_{21})]^{-1}$. The second field component $\hat{a}_2(t)$ is excited due to the interaction with atomic coherence at $t=t_o$. The third $\hat{a}_3(t)$ and fourth $\hat{a}_4(t)$ field components are excited by the bath modes $\hat{b}_2(\nu)$ and by the signal field $\hat{b}_1(t)$. Due to the initial state $|\Psi_{\rm in}(t)\rangle$, the field components $\hat{a}_2(t)$ and $\hat{a}_3(t)$ redetermine only the QED cavity vacuum without the excitation of real photons. By taking into account the expectation values $\langle\hat{b}_2^\dagger(\nu)\hat{b}_2(\nu)\rangle=\langle S_+^j(t_o)S_-^j(t_o)\rangle=0$ for the initial state, we leave only the nonvanishing term for the atomic coherence at $t=\tau$ determined by the signal field

$$\hat{S}_-^j(\tau)=-g_j^*\int_{t_o}^{\tau}dt'\Phi_j(\tau,t')\exp\{-i\Delta_j(\tau-t')\}\hat{a}_4(t'). \quad (13)$$

By using (13) and (3), we calculate the storage efficiency of the signal field $Q_{ST}(\tau)=\bar{P}_{ee}(\tau)/\bar{n}_1$ where $\bar{P}_{ee}(\tau)=\sum_{j=1}^{N}\langle S_+^j(\tau)S_-^j(\tau)\rangle$ is an excited level population of atoms after the interaction with last Mth signal field mode for $\tau>\tau_M+\delta t_M$ (we assume the usual relation for temporal duration and spectral width of the kth mode $\delta t_k\approx\delta\omega_k^{-1}$). The total number of photons in the input signal field is $\bar{n}_1=\sum_{k=1}^{M}\bar{n}_{1,k}$, $\bar{n}_{1,k}=\int_{-\infty}^{\infty}dt\langle\hat{b}_{1,k}^\dagger(t)\hat{b}_{1,k}(t)\rangle$ is a number of photons in the kth temporal mode, $\langle\cdots\rangle$ is a quantum averaging over the initial state $|\Psi_{\rm in}(t)\rangle$. Performing the algebraic calculations of $\bar{P}_{ee}(\tau)$, we find the quantum efficiency of storage $Q_{ST}=(1/\bar{n}_1)\sum_{k=1}^{n}Q_{ST,k}\bar{n}_{1,k}$ where the storage efficiency of the kth mode is

$$Q_{ST,k}=\int_{-\infty}^{\infty}d\nu Z(\nu,\Delta_{\rm tot},\Gamma_{\rm tot},\gamma_{1,2})\frac{\langle\hat{n}_{1,k}(\nu)\rangle}{\bar{n}_{1,k}}, \quad (14)$$

with spectral function

$$Z(\nu,\Delta_{\rm tot},\Gamma_{\rm tot},\gamma_{1,2}) = \frac{\Delta_{\rm tot}^2}{(\Delta_{\rm tot}^2+\nu^2)} \frac{4\gamma_1\Gamma_{\rm tot}}{|\gamma_1+\gamma_2+\frac{\Gamma_{\rm tot}}{(1-i\nu/\Delta_{\rm tot})}-2i\nu|^2}, \qquad (15)$$

where $\Gamma_{\rm tot}=2N|\bar{g}|^2/\Delta_{\rm tot}$ is a photon absorption rate by N-atomic ensemble in unit spectral domain within the IB line, $\Delta_{\rm tot}=\Delta_{\rm in}+\gamma_{21}$ is a total line width.

For relatively narrow spectral width $\delta\omega_k$ of the kth signal field and weak atomic decoherence rate in comparison with IB ($\delta\omega_k,\gamma_{21}\ll\Delta_{\rm tot}$), we get from Eqs. (14) and (15)

$$Q_{ST,k}=\frac{\gamma_1}{(\gamma_1+\gamma_2)}\frac{4\Gamma_{\rm tot}/(\gamma_1+\gamma_2)}{[1+\Gamma_{\rm tot}/(\gamma_1+\gamma_2)]^2}. \qquad (16)$$

Quantum efficiency $Q_{ST,k}$ reaches unity if the spectral function $Z(\nu=0,\Delta_{\rm tot},\Gamma_{\rm tot},\gamma_{1,2})=1$ that leads to the *matched impedance condition* $\Gamma_{\rm tot}/(\gamma_1+\gamma_2)=1$ when $\gamma_2/\gamma_1\ll 1$ (leading to $\Gamma_{\rm tot}\cong\gamma_1$) coinciding with the well-known matched impedance condition for simple absorption in a resonator [27,28]. $\gamma_2/\gamma_1\ll 1$ means a weakness of irreversible loss into the nonsignal modes. By taking into account $\Gamma_{\rm tot}=\gamma_1+\gamma_2$ we find spectral function $Z(\cdots)$ for arbitrary frequency ν

$$Z(\nu,\Delta_{\rm in},\Gamma_{\rm tot}=\gamma_1+\gamma_2) = \frac{\gamma_1}{\Gamma_{\rm tot}}\frac{1}{\left\{1+\frac{\nu^2}{\Gamma_{\rm tot}^2\Delta_{\rm tot}^2}\left[\frac{1}{4}(\Gamma_{\rm tot}-2\Delta_{\rm tot})^2+\nu^2\right]\right\}}. \qquad (17)$$

The spectral function $Z(\cdots)$ for various broadening widths $\Delta_{\rm tot}$ is depicted in Figs. 1 and 2 when the matched impedance condition is fulfilled. As seen from Eq. (17) and in Figs. 1 and 2, there is an optimal broadening width $\Delta_{\rm tot}=\Gamma_{\rm tot}/2$ (we call it *optimal spectral matching condition*) where $Z(\cdots)$ is close to unity in the broadest spectral range. It is connected with the fact that at this condition, the spectral function $Z(\cdots)$ is inversely proportional to the fourth degree of frequency ν^4 rather than the second.

The first optimal condition implies that radiation entering in the QED cavity will completely transfer to the atoms at resonant frequency ($\nu\approx 0$) since the IB atomic system absorbs the radiation with the optimal rate $\Gamma_{\rm tot}\cong\gamma_1$ leading to relation $\hat{a}(t)=\sqrt{\gamma_1}\hat{b}_1(t)$ for arbitrary temporal mode shape (however, in the limit of narrow spectral width) which also means an absence of the reflection of the input signal field from the QED cavity.

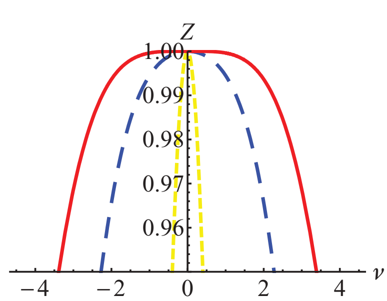

FIG. 1. (Color online) Spectral function $Z(\cdots)$ as a function of ν for various IBs from narrow to optimal spectral width: $\Delta_{\rm tot}=1$ (yellow, short dashed), $\Delta_{\rm tot}=3$ (blue, long dashed), $\Delta_{\rm tot}=5$ (red, solid); we use the units where $\Gamma_{\rm tot}=10$.

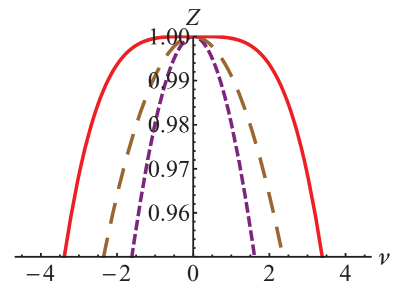

FIG. 2. (Color online) Spectral function $Z(\cdots)$ as a function of ν for IBs from optimal to infinite spectral width: $\Delta_{\rm tot}=5$ (red, solid), $\Delta_{\rm tot}=15$ (brown, long dashed), $\Delta_{\rm tot}/\Gamma_{\rm tot}\gg 1$ (purple, short dashed); we use the units where $\Gamma_{\rm tot}=10$.

The second optimal condition matches the spectral shapes of cavity window transparency with the IB of the atomic transition [29] near the central frequency. Thereby, the second condition provides almost perfect fulfillment of the first condition in the broadest spectral width of the light field modes. Thus, if both optimal matching conditions are held, we will get the broadest spectral range for perfect quantum storage of each input kth mode. We note that the maximum number of modes is limited only by $M_{\rm max}\sim\Delta_{\rm in}/\gamma_{21}\gg 1$ and the storage of the multimode field in IB atomic system will occur by one step procedure.

IV. MULTIMODE QUANTUM MEMORY

In accordance with the original protocol of photon echo QM [10], after the complete absorption of the signal QM on the IB transition, we recover the dephased atomic coherence by changing the frequency detunings of atoms at time moment $t=\tau$. In general, the inversion of the atomic detunings $\Delta_j\rightarrow -\Delta_j$ can be done by using a Doppler effect [10], properties of local fields [11], or by directly changing a polarity of the external magnetic or electric fields [12,13] in the cases where the IBs are determined by Zeeman or Stark effects in external control fields. It is also possible to recover the dephased atomic coherence with quite large efficiency by exploiting the atomic frequency comb structure of the IB line [30]. Below we assume that the IBs are caused by the Stark or Zeeman effects that are more convenient for the analyzed scheme of QM in the QED cavity.

At first by using a Schrödinger picture we demonstrate the QM in QED cavity in a most general way. Here, in spite of a huge complexity of the compound light-atoms system, we show that their quantum dynamics governed by H_1 in (2) can be perfectly reversed in time by our demand in a simply robust way. That is by transferring to the new field operators $\hat{a}=-\hat{A}$ and $\hat{b}_1(\omega_o-\Delta\omega)=\hat{B}_l(\omega_o+\Delta\omega)$ (with similar relations for the Hermit conjugated operators), we get a new Hamiltonian with an opposite sign in comparison with the initial one $\hat{H}_1'=-\hat{H}_1$ determining a temporally reversed evolution $\hat{U}_2[(t-\tau)]=\exp\{-i\hat{H}_1'(t-\tau)/\hbar\}=\exp\{i\hat{H}_1(t-\tau)/\hbar\}$. Ignoring now a weak interaction with the bath (nonsignal) modes and slow atomic decoherence, i.e., assuming $\gamma_{21}\approx 0$, $\gamma_2\approx 0$, respectively, we find that the quantum evolution $\hat{U}_2$ recovers the initial quantum state of the multimode signal field and atoms at $t=2\tau$ due to unitary reversibility of the echo signal emission making the echo field spectrum inverted relatively to the central frequency ω_o in comparison with the original one.

Coming back to the real parameters of the atomic decoherence rate γ_{21} and cavity parameters γ_1, γ_2, we analyze below a retrieval of the echo field and QM efficiency for the multimode signal field (the field index "e" is introduced to indicate the echo emission stage). By changing $\Phi_j^{(s)}(p)$ to $\Phi_j^{(e)}(p) = \int_\tau^\infty dt \exp\{-(p - i\Delta_j)(t-\tau)\}\Phi_j(t,\tau)$, we find the Laplace image of the quantum echo field irradiated by the atomic coherence $\hat{S}_-^j(\tau)$ in accordance with Eq. (9). We find the echo field in time domain picture $\hat{a}_e(t)$ after inverse Laplace transformation, a calculation of all temporal integrals and summation over the atomic responses. By taking into account large IB in comparison with the atomic decoherence rate $\Delta_{\text{in}} \gg \gamma_{21}$, we find the echo field irradiated in the QED cavity

$$\hat{a}_e(t) = -\frac{\exp\{-2\gamma_{21}(t-\tau)\}}{\sqrt{\gamma_1}}\int_{-\infty}^{+\infty}\frac{d\nu}{\sqrt{2\pi}} \times \sum_{k=1}^{M} Z(\nu,\Delta_{\text{in}},\Gamma_{\text{in}})\hat{b}_{1,k}(\nu)\exp\{i\nu(t+\tau_k-2\tau)\}, \tag{18}$$

where $\Gamma_{\text{in}} = 2N|\bar{g}|^2/\Delta_{\text{in}} \approx \Gamma_{\text{tot}}$ and we have assumed that $\gamma_{21}\delta t_k \ll 1$.

The total photon number operator of the echo field signal irradiated at time $t \gg 2\tau$ is $\hat{n}_e = \int_{-\infty}^{\infty} d\nu \hat{b}_e^\dagger(\nu)\hat{b}_e(\nu) = \sum_{k=1}^{M}\hat{n}_{e,k}$, where $\hat{n}_{e,k} = \gamma_1\int_\tau^\infty dt'\hat{a}_{e,k}^\dagger(t')\hat{a}_{e,k}(t')$ relates to the kth field mode with average photon number $\langle\hat{n}_{e,k}\rangle = \exp\{-4\gamma_{21}(\tau-\tau_k)\}Q_{ME,k}\bar{n}_{1,k}$ and

$$Q_{ME,k} = \int_{-\infty}^{+\infty} d\nu[Z(\nu,\Delta_{\text{in}},\Gamma_{\text{in}},\gamma_{1,2})]^2\frac{\langle\hat{n}_{1,k}(\nu)\rangle}{\bar{n}_{1,k}}. \tag{19}$$

By comparing (19) with the storage efficiency (14), we find that the complete spectral function of QM $[Z(\nu,\Delta_{\text{in}},\Gamma_{\text{in}})]^2$ is filtering the input light spectrum in the echo field that demonstrates an influence of two similar steps of the light-atoms interaction in accordance with their temporal reversibility; the factor $\exp\{-4\gamma_{21}(\tau-\tau_k)\}$ is a result of the irreversible atomic decoherence on the QM efficiency during the storage time $2(\tau-\tau_k)$ of the th mode. $Q_{ME,k}$ for the Lorentzian spectral shape of each kth temporal field mode $\langle\hat{n}_{1,k}(\nu)\rangle = \langle\hat{b}_1^\dagger(\nu)\hat{b}_1(\nu)\rangle_k = \frac{1}{\pi}\bar{n}_{1,k}\delta\omega_k/(\delta\omega_k^2+\nu^2)$ and for Gaussian shape $\langle\hat{n}_{1,k}(\nu)\rangle = \bar{n}_{1,k}\frac{\delta\omega_k}{\sqrt{2\pi}}\exp\{-\frac{\nu^2}{2\delta\omega_k^2}\}$ are presented in Fig. 3. We had seen that the quantum efficiency $Q_{ME,k}$ is higher for an input light field with a Gaussian spectrum because of the weaker character of its spectral wings for $|\nu| > \delta\omega_k$.

Total quantum efficiency Q_{ME} of the multimode field retrieval is

$$Q_{ME} = \frac{1}{\bar{n}_1}\sum_{k=1}^{M}\exp\{-4\gamma_{21}(\tau-\tau_k)\}Q_{ME,k}\bar{n}_{1,k}. \tag{20}$$

The quantum efficiency of the multimode field retrieval for Lorentzian and Gaussian spectral shapes of the field modes are depicted in Fig. 4 in accordance with Eqs. (18) and (19) for a broad range of ratios $\Gamma_{\text{in}}/(\gamma_1+\gamma_2)$ and reasonable parameters of the IB resonant atoms.

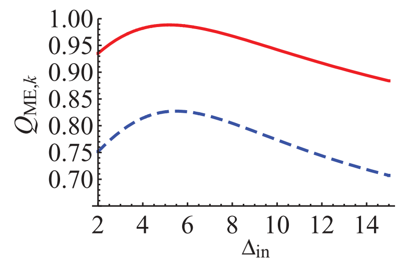

FIG. 3. (Color online) Quantum memory efficiency $Q_{ME,k}$ for kth mode with Gaussian spectral shape $\sim \frac{\delta\omega_k}{\sqrt{2\pi}}\exp\{-\frac{\nu^2}{2\delta\omega_k^2}\}$ (red, solid) and with Lorentian spectral shape $\sim \frac{1}{\pi}\bar{n}_{1,k}\delta\omega_k/(\delta\omega_k^2+\nu^2)$ (blue, dashed), the calculations have been done in units of $\delta\omega_k = 1$ for $\Gamma_{\text{tot}} = 10$. It is seen that $Q_{ME,k}$ reaches maximum at $\Delta_{\text{in}} = \Gamma_{\text{tot}}/2$.

As seen in Fig. 4, the QM efficiency is very close to unity at the optimal atomic and cavity parameters $\Gamma_{\text{in}}/(\gamma_1+\gamma_2) = 1$ for the Gaussian spectrum (upper curve) characterized by the spectral width which is close to the width of the Lorentzian spectral shape (down curve). Such high QM efficiency is possible for the Gaussian spectrum only at the condition *of optimal spectral matching* $\Gamma_{\text{in}} = 2\Delta_{\text{in}} = 10$ even for relatively narrow IB width $\Delta_{\text{in}}/\delta\omega = 5$. Otherwise, the QM efficiency can be close to unity only in the limit $\gamma_1,\Delta_{\text{in}} \gg \delta\omega_k$, i.e., for a too large light field temporal duration even if $\Gamma_{\text{in}} = \gamma_1$ and $\gamma_2 \ll \gamma_1$.

The optimal condition for the QM efficiency leads to the optimal optical depth of the resonant transition $\alpha L \sim \gamma_1 L/c$ (where c is the speed of light) that yields almost 100% QM efficiency even for thin optical depth. To give an example, we consider an optical cavity in Fig. 5.

$L = 1$ mm and $\gamma_1 = T/(2L/c) = 10^8$ s^{-1} for transmission coefficient $T = (2/3)\times 10^{-3}$ of the input mirror (where the second mirror of cavity has 100% reflectivity) that leads to the optimal optical depth $\alpha L \approx 3\times 10^{-4}$. Such small but optimal optical depth can be prepared by spectral tailoring of the original IB resonant line of rare-earth ions in the dielectric

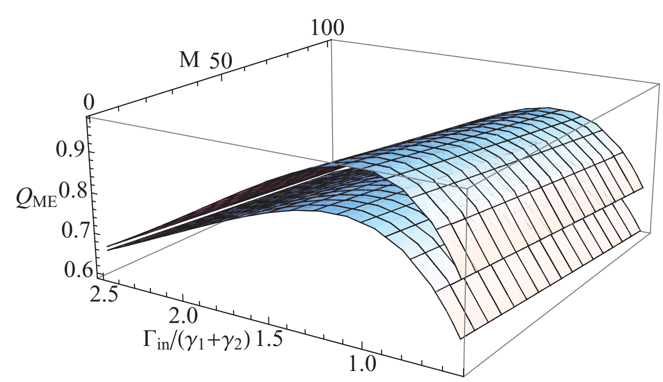

FIG. 4. (Color online) Quantum efficiency Q_{ME} for Gaussian (upper curve) and Lorentzian (down curve) spectral shapes of the input light fields as a function of the mode number $M := \{1,\ldots,100\}$ and of the ratio $\Gamma_{\text{in}}/(\gamma_1+\gamma_2)$ for the cavity with $\gamma_1+\gamma_2 = 10$, $\gamma_2/\gamma_1 = 0.01$ and atomic parameters: $\Delta_{\text{in}} = 5$, $\gamma_{21} = 0.0001$ which are given in units of spectral width $\delta\omega_k = \delta\omega = \delta t^{-1} = 1$ of the input signal mode; time delay between the nearest two temporal modes is $(\tau_{k+1}-\tau_k)/\delta t = 5$, each mode contains $\bar{n}_{1,k} = 1$ photon.

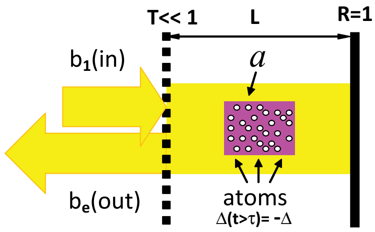

FIG. 5. (Color online) Optical scheme of the QM with one-sided QED cavity. First input semitransparent mirror has a transmission coefficient $T \ll 1$, a second mirror has 100% reflectivity ($R = 1$); $\gamma_1 = T/(2L/c)$, L is a longitudinal size of the cavity, c is the speed of light, $b_1(in)$, $b_e(out)$ are the input and echo fields, a is a cavity mode field; central box is a medium with atoms, the atomic frequency detunings are inverted at $t = \tau$.

crystals [5,13,17]. At last we note that it is a one-sided character of the cavity that provides a perfect storage and retrieval of the input light fields with 100% efficiency.

V. CONCLUSION

We have found that an efficient multimode photon echo QM can be realized in the QED cavity. Here, high QM efficiency can be constructed for the signal light field of sufficiently narrow spectral width (while for its arbitrary temporal shape) even for the atomic system with thin optical depth determined by the matching conditions for the IB resonant line of atoms and single cavity mode. We stress a principle advantage of the proposed multimode photon echo QM in a QED cavity with respect to the QMs based on well-known EIT or early variants of photon echo QMs [5] where 100% efficiency occurred only for the infinite optical depth of the coherent resonant atomic system ($\alpha L \gg 1$). Also, we have to note that the fidelity of the analyzed photon echo QM scheme will be close to unity if we take into account the temporally reversed shape of the irradiated light fields. (The most recent applicable analysis of the fidelity for photon echo QM of single photon fields is given in [31].) So, using the QED cavity not only increases the optical depth via the well-known Purcell factor [32], but makes it possible to realize optimal conditions for an interaction between the external field and atoms. The first condition is the *matched impedance condition* and the second one is the *spectral matching condition*. Concerning the second condition, we anticipate that a delicate spectral tailoring of the inhomogeneous broadening can provide a high efficiency QM even in rather broad spectral range. The possibility predicted here to get a highest efficiency for the QM at finite values of the experimental parameters is easily achievable in practice and its multimode character opens a door for real applications in particular for the construction of quantum repeater.

ACKNOWLEDGMENTS

The work was supported by Russian Foundation of Basic Research Grants No. 08-07-00449 and No. 10-02-01348.

[1] H.-J. Briegel, W. Dür, J. I. Cirac, and P. Zoller, Phys. Rev. Lett. **81**, 5932 (1998).
[2] M. A. Nielsen and I. L. Chuang, *Quantum Computation and Quantum Information* (Cambridge University Press, Cambridge, 2000).
[3] P. Kok *et al.*, Rev. Mod. Phys. **79**, 135 (2007).
[4] A. I. Lvovsky, B. C. Sanders, and W. Tittel, Nature Photonics **3**, 706 (2009).
[5] W. Tittel, M. Afzelius, T. Chaneliére, R. L. Cone, S. Kröll, S. A. Moiseev, and M. Sellars, Laser Photon. Rev. **4**(2), 244 (2010).
[6] M. Fleischhauer and M. D. Lukin, Phys. Rev. Lett. **84**, 5094 (2000).
[7] A. V. Gorshkov, A. Andre, M. Fleischhauer, A. S. Sorensen, and M. D. Lukin, Phys. Rev. Lett. **98**, 123601 (2007).
[8] I. Novikova, A. V. Gorshkov, D. F. Phillips, A. S. Sorensen, M. D. Lukin, and R. L. Walsworth, Phys. Rev. Lett. **98**, 243602 (2007).
[9] J. Appel, E. Figueroa, D. Korystov, M. Lobino, and A. I. Lvovsky, Phys. Rev. Lett. **100**, 093602 (2008).
[10] S. A. Moiseev and S. Kröll, Phys. Rev. Lett. **87**, 173601 (2001); S. A. Moiseev and B. S. Ham, Phys. Rev. A **70**, 063809 (2004).
[11] S. A. Moiseev, V. F. Tarasov, and B. S. Ham, J. Opt. B: Quantum Semiclass. Opt. **5**, S497 (2003).
[12] B. Kraus, W. Tittel, N. Gisin, M. Nilsson, S. Kroll, and J. I. Cirac, Phys. Rev. A **73**, 020302 (2006).
[13] A. L. Alexander, J. J. Longdell, M. J. Sellars, and N. B. Manson, Phys. Rev. Lett. **96**, 043602 (2006); G. Hétet, J. J. Longdell, A. L. Alexander, P. K. Lam, and M. J. Sellars, *ibid.* **100**, 023601 (2008).
[14] J.-L. Le Gouët and P. R. Berman, Phys. Rev. A **80**, 012320 (2009).
[15] C. Simon, H. de Riedmatten, M. Afzelius, N. Sangouard, H. Zbinden, and N. Gisin, Phys. Rev. Lett. **98**, 190503 (2007).
[16] J. Nunn, K. Reim, K. C. Lee, V. O. Lorenz, B. J. Sussman, I. A. Walmsley, and D. Jaksch, Phys. Rev. Lett. **101**, 260502 (2008).
[17] I. Usmani *et al.*, e-print arXiv:1002.3782v1 [quant-ph].
[18] S. A. Moiseev and M. I. Noskov, Laser Phys. Lett. **1**, 303 (2004).
[19] N. Sangouard, C. Simon, M. Afzelius, and N. Gisin, Phys. Rev. A **75**, 032327 (2007).
[20] M. Fleischhauer, S. F. Yelin, and M. D. Lukin, Opt. Commun. **179**, 395 (2000).
[21] A. V. Gorshkov, A. Andre, M. D. Lukin, and A. S. Sorensen, Phys. Rev. A **76**, 033804 (2007).
[22] T. Wang, C. Greiner, and T. W. Mossberg, Opt. Lett. **23**, 1736 (1998).
[23] S. A. Moiseev, e-print arXiv:quant-ph/0605035.
[24] A. V. Gorshkov, T. Calarco, M. D. Lukin, and A. S. Sorensen, Phys. Rev. A **77**, 043806 (2008).

[25] D. F. Walls and G. J. Milburn, *Quantum Optics* (Springer, Heidelberg, 1994).
[26] M. Tavis and F. W. Cummings, Phys. Rev. **170**, 379 (1968).
[27] H. A. Haus, *Waves and Fields in Optoelectronics* (Prentice-Hall, Inc., Englewood Cliffs, NJ, 1984), Sec. 5.5.
[28] A. E. Siegman, *Lasers* (University Science Books, Mill Valley, CA, 1986), p. 1285.
[29] We use a Lorentzian IB of atomic transition only for simplicity of the calculations and this effect will occur for Gaussian and other IB shapes characterized by the quadratic behavior ν^2 near to central atomic frequency.
[30] H. de Reidmatten *et al.*, Nature (London) **456**, 773 (2008).
[31] S. A. Moiseev and W. Tittel, Phys. Rev. A **82**, 012309 (2010).
[32] E. M. Purcell, Phys. Rev. **69**, 681 (1946).